

Raman Amplification: An Enabling Technology for Long-Haul Coherent Transmission Systems

Wayne S. Pelouch, *Member, IEEE*

(Tutorial Review)

Abstract—Raman amplification has been commercially utilized in optical transmission systems for more than a decade. The drive toward higher spectral density has increased the interest in Raman to improve system performance. This tutorial reviews the benefits of Raman amplification, defines methods to analyze system performance, and describes the issues involved with system deployment and operation.

Index Terms—Coherent communications, distributed amplifiers, optical fiber amplifiers, optical fiber communications, optical fiber networks, Raman scattering.

I. INTRODUCTION

THE past 15 years have seen an incredible increase in data rates of optical transponders and, more recently, a move to multi-level phase modulated formats and coherent digital signal processing at the receiver. However, the fiber optic transport system has not changed much over this time and is dominated by C-band erbium-doped fiber amplifiers (EDFAs). These amplifiers are the main building blocks of the transport system that define the performance characteristics of the optical network independent of the transponders. The improvements in transponder technology, including powerful forward error correction (FEC) codes, have allowed data rates to increase without requiring a significant improvement in the transport system.

The advances in FEC and modulation format have kept pace with the bit rate from 2.5 to 100 Gb/s as depicted in Fig. 1 and which shows the FEC technology (G-FEC, Enhanced FEC, Soft-Decision FEC) and modulation format (On-Off Keying, Differential Phase-Shift Keying, Polarization-Multiplexed Differential Quadrature Phase-Shift Keying, Polarization-Multiplexed Non-Differential 8 and 16 Quadrature-Amplitude Modulation) employed at each bit rate. However, steps beyond 100 Gb/s at higher spectral efficiency are requiring a higher optical signal-to-noise ratio (OSNR) in the fiber plant as shown by the solid arrow (100 to 150 to 200 Gb/s).

Optical fiber technology has also improved with lower attenuation and larger effective core area, but the vast amount of installed fiber requires a step improvement in the transport system to maintain the trend to higher data capacity. Raman amplification is a key technology for improving the performance of

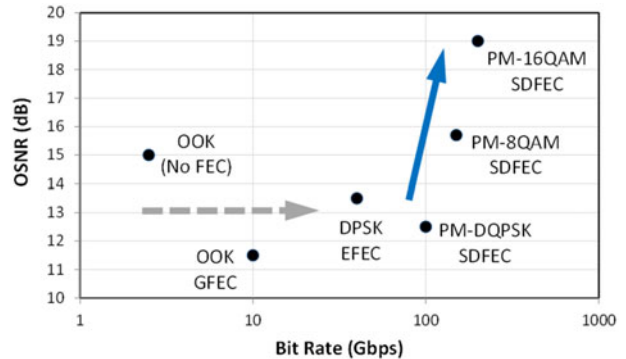


Fig. 1. Improvements in transponder technology from 2.5 to 200 Gb/s. FEC and modulation format advancements have kept the OSNR requirements below the 2.5 Gb/s threshold (dashed arrow), but the current trend in higher spectral density has resulted in higher OSNR requirements (solid arrow).

fiber optic transport systems to accommodate the higher OSNR requirement. A likely next step in the drive to higher data capacity at the same OSNR would be to move beyond the C-band. The flexible spectral characteristics of Raman systems are compatible with a wideband transmission window (up to 100 nm wide).

The technology inherent to Raman amplification has not changed appreciably in the last decade, although there has been a continual improvement in laser diode power levels and reliability which are critical features of Raman amplifiers. Prior overviews of Raman amplification [1]–[3] provide an excellent treatment of the basics of Raman amplification, history, and related optical effects. This tutorial will briefly summarize the fundamentals and in more detail discuss the methods to analyze Raman amplification in coherent networks, list some general scaling laws for large effective area fiber, and describe the issues involved with system deployment and operation. This paper is based on a tutorial presentation given at the 2015 Optical Fiber Communications (OFC) conference [4].

II. RAMAN AMPLIFICATION

A. Background

Raman amplification occurs due to an inelastic scattering of optical radiation with molecular vibrations in a material [5]. The scattered “Stokes” waves are at a lower energy, or longer wavelength, than the incident optical radiation. The driving optical field is typically called the “pump” and the scattered light, the “signal.” The excited molecules when driven by the pump light can be stimulated to emit when input light at the signal wave-

Manuscript received May 29, 2015; revised July 15, 2015; accepted July 16, 2015. Date of publication July 19, 2015; date of current version January 24, 2016.

The author is with the Xtera Communications, Allen TX 75013 USA (e-mail: wayne.pelouch@xtera.com).

Color versions of one or more of the figures in this paper are available online at <http://ieeexplore.ieee.org>.

Digital Object Identifier 10.1109/JLT.2015.2458771

length is present resulting in a coherent amplification process at the signal wavelengths. The Raman gain coefficient of this process is related to the scattering cross section which is material dependent.

The equations that govern the Raman process for a single co-polarized pump wavelength and signal wavelength travelling in the same direction are (neglecting spontaneous noise) [6]

$$\frac{dP_s}{dz} = \frac{g_R}{A_{\text{eff}}} P_s P_p - \alpha_s P_s \quad (1)$$

$$\frac{dP_p}{dz} = -\frac{\nu_p}{\nu_s} \frac{g_R}{A_{\text{eff}}} P_p P_s - \alpha_p P_p \quad (2)$$

where P_s and P_p are the signal and pump powers, respectively; g_R is the Raman gain coefficient; A_{eff} is the effective area of the modes in the fiber; α_s and α_p are the fiber attenuation coefficients for the signal and pump, respectively; ν_s and ν_p are the signal and pump frequencies, respectively; and z is the propagation length variable. The term ν_p/ν_s accounts for the fact that one pump photon is depleted for each signal photon created (i.e., the quantum efficiency). In (1) and (2) A_{eff} is explicitly shown such that the scaling with fiber core area may be seen. The quantity (g_R/A_{eff}) (which includes the effects of signal-pump mode overlap) has units of $1/(W \cdot \text{km})$. Raman gain is polarization dependent with very low interaction between orthogonally polarized signal and pump.

The equations may be solved analytically with the condition that the pump power is not depleted by the signal as a function of distance through fiber. Under this “small signal” assumption, the signal gain is

$$\begin{aligned} \text{total gain} &= \frac{P_s(L)}{P_s(0)} \\ &= e^{-\alpha_s L} \exp[P_p(0) \cdot L_{p,\text{eff}} \cdot g_R/A_{\text{eff}}] \quad (3) \end{aligned}$$

$$L_{p,\text{eff}} = (1 - e^{-\alpha_p L})/\alpha_p \quad (4)$$

where $L_{p,\text{eff}}$ is called the effective interaction length of the pump and is about 17 km in SMF for a pump wavelength of 1450 nm. A significant amount of Raman gain occurs up to about twice $L_{p,\text{eff}}$, so this should not be considered to be the length of fiber required to achieve the calculated gain. The term $\exp(-\alpha_s L)$ is the fiber transmission, or inverse of the fiber loss. The second exponential in (3) is the Raman gain not including the span transmission, sometimes called the “on/off” gain. This is what shall be referred to as Raman gain in the rest of this article.

If we convert the gain equation (3) to dB units, then it can be seen that Raman gain in dB is proportional to the product of pump power in W, L_{eff} in km, and (g_R/A_{eff}) . The Raman gain coefficient as defined above, g_R , is similar in all silica-based fibers and varies in different fiber types due to different doping profiles and mode overlap with these dopants [7], [8]. The spectral shape of g_R depends on the difference in pump and signal frequencies ($\nu_p - \nu_s$) and the magnitude of g_R depends on the absolute pump frequency, ν_p [9]. The factor $(1/A_{\text{eff}})$ accounts for the majority of variation of Raman gain in different fibers. Plots of (g_R/A_{eff}) are shown in Fig. 2 for common fiber types at a pump wave-length of 1420 nm and the scaling versus ν_p is shown in Fig. 3.

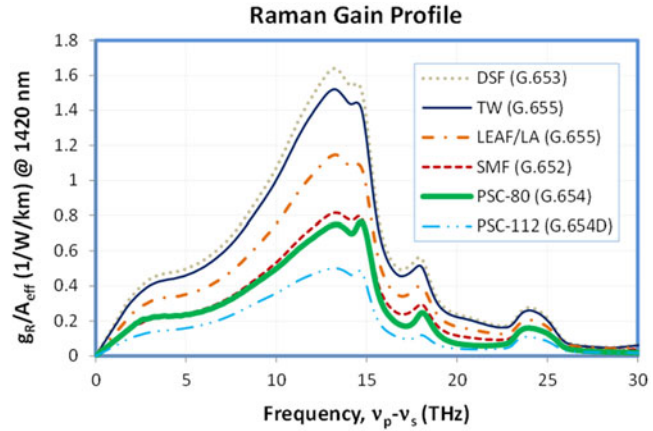


Fig. 2. Raman gain spectral shape for different fiber types at a pump wavelength of 1420 nm. For pure-silica core fibers (PSC), two different effective core areas at 1550 nm are also shown (80 and $112 \mu\text{m}^2$).

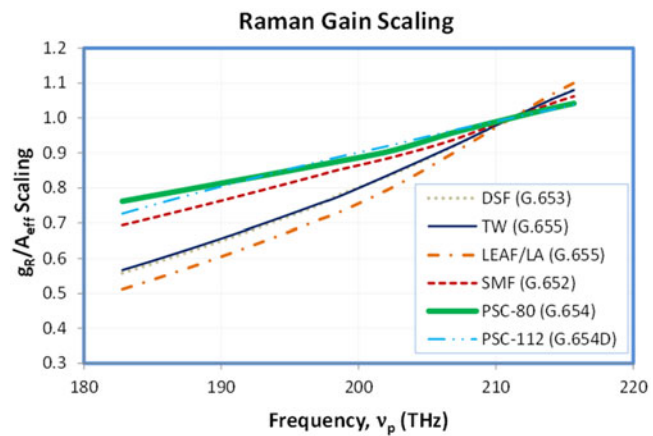


Fig. 3. Raman gain magnitude scaling versus pump frequency (relative to 1420 nm pump) for different fiber types.

B. General Raman Equations

The case of multiple pumps and signals propagating in either direction is characterized by a set of coupled equations that can be written in a compact form as

$$d_i \frac{dP_i}{dz} = -\alpha_i P_i + \sum_j (P_j + N_{ij}) g_{ij} P_j \quad (5)$$

$$g_{ij} = \begin{cases} g_R(\nu_j, \nu_j - \nu_i)/(2 \cdot A_{\text{eff}}) & \nu_j > \nu_i \\ 0 & \nu_j = \nu_i \\ -(\nu_i/\nu_j) \cdot g_R(\nu_i, \nu_i - \nu_j)/(2 \cdot A_{\text{eff}}) & \nu_j < \nu_i \end{cases} \quad (6)$$

$$N_{ij} = 2h\nu_i \Delta\nu_i (1 + n_{ij}),$$

$$n_{ij} = \left[\exp\left(\frac{h |\nu_j - \nu_i|}{k_B T}\right) - 1 \right]^{-1} \quad (7)$$

where the subscripts i and j run over all signals and pumps, d_i is the direction ($= \pm 1$ for forward/backward propagation), h is Planck's constant, k_B is Boltzmann's constant, and T is the temperature. The factor of 2 in (6) and (7) accounts for the pump having equal power in the two possible polarization states in a fiber. The noise source term, N_{ij} , can generally be

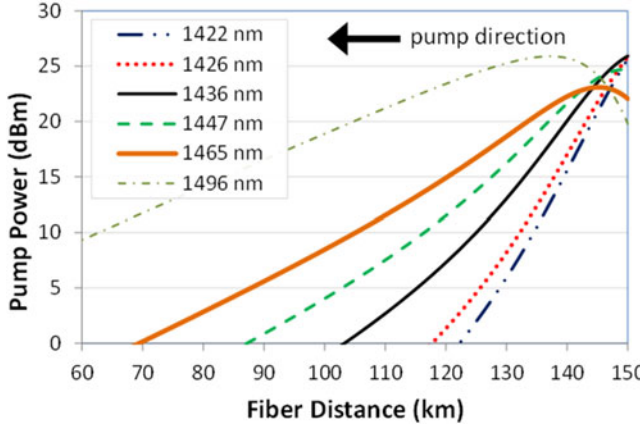


Fig. 4. Pump profiles (backward propagating) in 150 km SMF. The pumps are in order of increasing wavelength in the legend, ranging from 1422 to 1496 nm.

ignored except for calculating the spontaneous noise spectrum which is modeled as extra signals with zero input power over a range of frequencies. The term n_{ij} in (7) is the Boltzmann's thermal occupancy factor for phonons and is equal to 0.138 at $T = 300$ K and $|\nu_j - \nu_i| = 13.2$ THz (which is the peak of the Raman gain curve). However, for Raman interactions with multiple pumps and signals, some of the pumps may be closer to some of the signals resulting in a higher noise term ($n_{ij} = 0.534$ at $|\nu_j - \nu_i| = 6.6$ THz). In either case, N_{ij} does not result in enough power to deplete the pumps in most situations and may be ignored when solving for gain.

The propagation equations indicate that all of the signal and pump powers are coupled such that any shorter wavelength is a “pump” for any longer wavelength. Thus, even without high power Raman pumps, there is a Raman effect if multiple signals propagate through a fiber resulting in some transfer of power from short to long wavelengths. Additionally, there is a transfer of power between multiple pump laser wavelengths which is depicted in Fig. 4 for the case of six pumps with wavelengths from 1422 to 1496 nm. Note that the longest wavelength pump starts (at 150 km) at the lowest power but increases in power over the first 15 km (to 135 km) while the shortest wavelength pump depletes the quickest (transferring power to longer wavelength pumps).

This pump-to-pump power transfer can be utilized in “higher order” Raman pumping configurations [10] where the frequency difference between the longest and shortest wavelength pump may exceed one Stokes shift. The first third-order Raman system [11] utilized a fiber laser to generate pump wavelengths as low as 1276 nm. The goal of this technique is to push the longest wavelength pump power further into the fiber and minimize the variation in signal power within the line fiber which further minimizes nonlinear effects, MPI, and optical noise [12].

The general Raman equations may only be solved numerically, but simple scaling laws still exist. Even for multiple-pump Raman amplification, the total Raman gain in dB is proportional to total pump power in Watts as depicted in Fig. 5. Two fiber attenuation values are shown for each fiber type with lower attenuation (larger $L_{p,\text{eff}}$) resulting in higher gain. The scal-

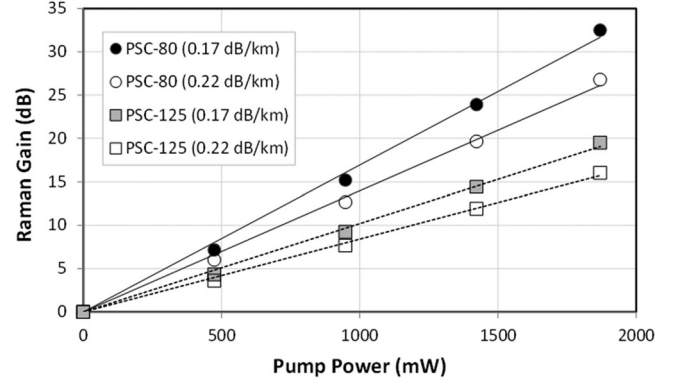


Fig. 5. Average Raman gain (dB) across the C-band versus pump power (mW) for pure-silica core fiber at two different A_{eff} (in μm^2) and α_s (dB/km) values (in parentheses). Three pumps (1422, 1432, 1452 nm) are adjusted simultaneously.

ing versus A_{eff} can be compared by looking at 1500 mW of pump power and 0.17 dB/km of fiber attenuation where the $80 \mu\text{m}^2$ PSC fiber (PSC-80) has about 25 dB gain and the $125 \mu\text{m}^2$ PSC fiber (PSC-125) has about 15 dB gain. (There is some slight difference in mode overlap with the core which accounts for the difference in the ratios 80/125 and 15/25.) The calculated gain in Fig. 5 is for wide-band (C- + L-band) amplification which requires more pump power than amplification only within the C-band.

III. RAMAN AMPLIFICATION BENEFITS

One obvious benefit of distributed Raman amplification is the gain itself, but the more important benefit is the lower noise that accompanies that gain compared to lumped amplification. The noise is defined at the optical receiver where the signal-to-noise ratio (SNR) defines the bit error rate of the data transmission. The changes in SNR after passing through an amplifier is further quantified by the noise figure (NF) which is the ratio of input to output SNR. In the optical domain, an optical SNR (OSNR) is defined as the ratio of optical signal power to optical noise (often referred to as “amplified spontaneous emission” or ASE) within a reference bandwidth, $\Delta\nu$. The equations for OSNR and NF are [14]

$$\text{OSNR} = \frac{P_s}{\rho_{\text{ASE}} \Delta\nu}, \quad \text{NF} = \left(\frac{\rho_{\text{ASE}}}{h\nu_s} + 1 \right) \frac{1}{G} \quad (8)$$

where ρ_{ASE} is the optical noise density (W/Hz) and G is the linear gain. It will also be important to understand how the NF accumulates with multiple loss and gain elements and is given by [15]

$$\text{NF}_{\text{total}} = \text{NF}_1 + \frac{\text{NF}_2 - 1}{G_1} + \frac{\text{NF}_3 - 1}{G_1 G_2} + \dots \quad (9)$$

where NF_i and G_i are the linear NF and gain of the i^{th} element.

There are a number of different configurations in which Raman can be utilized on a fiber span. The Raman pumps may be counter-propagating with respect to the signal (backward Raman) and/or co-propagating with the signal (forward Raman) and, additionally, residual pump power from Raman can power

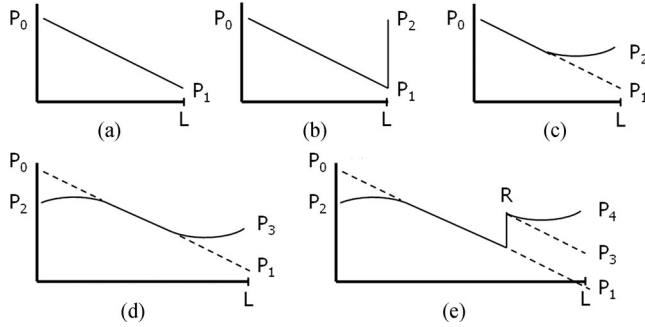


Fig. 6. Signal power profiles (dBm) for different span amplification schemes in a span of length L (km) and span loss $L_{\text{span}} = \exp(\alpha_s L)$. Dashed lines show power profiles without Raman amplification (not to scale). (a) span, (b) EDFA, (c) Bkwd Raman, (d) Fwd + Bkwd Raman, (e) Fwd + Bkwd Raman + ROPA.

a remotely-pumped optical amplifier (ROPA). A ROPA is typically some Erbium-doped fiber placed between 60 and 140 km from the equipment node and basically performs the function of an EDFA mid-span. In Fig. 4 it can be seen that the longest wavelength Raman pump has almost 10 dBm (10 mW) of power at a distance of 90 km from the backward Raman node (at 60 km on the plot which is 90 km from the Raman pumps located at 150 km). This residual pump power could be used to pump a ROPA at that location with >20 dB of gain. Higher order Raman pumping can increase the distance of the ROPA from the Raman pumps which is particularly useful for unrepeated Raman systems [13]. Fig. 6 shows different signal power profiles for different amplification schemes, each of which will be analyzed. The baseline comparison case is a fiber span with an EDFA at the end with its gain set to the preceding span loss [see Fig. 6(b)].

A. Baseline EDFA-Only Amplification

A fiber span without amplification [see Fig. 6(a)] generates no ASE and thus from (8) has a NF of $1/G = (P_0/P_1) = \exp(\alpha_s \cdot L)$ which is the span loss (L_{span}). The NF of a fiber span with an EDFA [see Fig. 6(b)] is calculated from (9) and is equal to

$$\text{NF}_{\text{total}} = L_{\text{span}} \cdot \text{NF}_{\text{EDFA}}. \quad (10)$$

In dB units this is just the sum of the span loss in dB and the EDFA NF in dB (which is typically 4.5 to 6 dB).

B. Backward Raman Amplification

A fiber span with backward Raman has a NF that can be calculated by noting [see Fig. 6(c)] that $1/G = P_0/P_2 = (P_0/P_1) \cdot (P_1/P_2) = (L_{\text{span}}) \cdot (1/G_{\text{BR}})$, where G_{BR} is the backward Raman gain excluding span loss. The NF is then $\text{NF}_{\text{span}} = L_{\text{span}} \cdot \text{NF}_{\text{BR}}$ where NF_{BR} is the NF of the backward Raman in the fiber span excluding the span loss (sometimes referred to as the “effective NF”)

$$\text{NF}_{\text{span}} = L_{\text{span}} \cdot \text{NF}_{\text{BR}}, \quad \text{NF}_{\text{BR}} = \left(\frac{\rho_{\text{ASE}}}{h\nu_s} + 1 \right) \frac{1}{G_{\text{BR}}}. \quad (11)$$

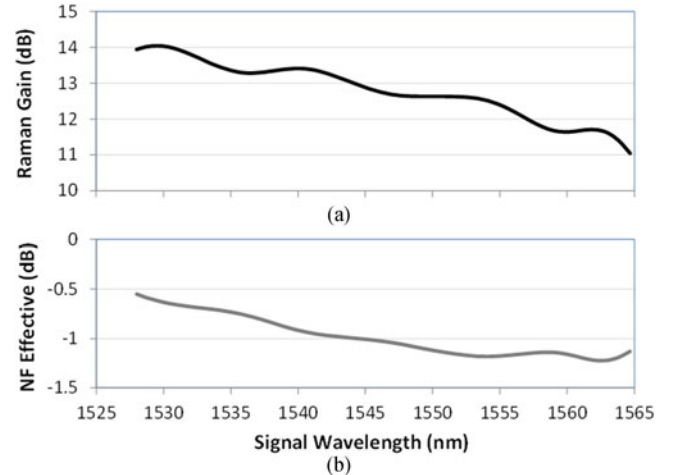


Fig. 7. (a) Raman gain (dB) and (b) Effective NF (NF_{BR} , dB) for three backward Raman pumps totaling 650 mW in SMF in the C-band.

The ρ_{ASE} of a span with backward Raman can be approximated with an analytical formula [16], [17]. However, for multiple Raman pumps an accurate calculation of NF_{BR} requires solving (5)–(7). A plot of the Raman gain and effective NF are shown in Fig. 7 for the case of 650 mW and three backward Raman pumps within the C-band. If we assume the span with Raman is followed by an EDFA, then the total NF is

$$\text{NF}_{\text{total}} = L_{\text{span}} \left[\text{NF}_{\text{BR}} + \frac{\text{NF}_{\text{EDFA}} - 1}{G_{\text{BR}}} \right] \quad (12)$$

where NF_{EDFA} is the NF of the EDFA. The effect of NF_{EDFA} is reduced due to the preceding Raman gain. For $\text{NF}_{\text{EDFA}} = 4.5$ dB, the total NF is about -0.25 to -0.52 dB plus the span loss (in dB) for the example of Fig. 7. Thus, the OSNR benefit from backward Raman is about 4.75 dB better than with an EDFA-only span which is about a factor of 3 in linear units. Thus, with the backward Raman gain of Fig. 7, optical transmission over three times the distance is possible at the same OSNR as without backward Raman.

C. Forward Raman Amplification

Forward Raman is typically only used with backward Raman with a power profile shown in Fig. 6(d). The ASE density generated at the front of the span gets attenuated by the span loss and is therefore small compared to ASE generated at the end of the span by backward Raman (and/or the EDFA). In the limit of larger span loss (which is the only case where forward Raman is typically applied), then the forward Raman NF is approximately $1/G_{\text{FR}}$, where G_{FR} is the forward Raman gain excluding span loss ($G_{\text{FR}} = P_0/P_2$ in Fig. 6(d)). Thus, effectively the span loss is just reduced by the forward Raman gain. The total NF including both forward and backward Raman and an EDFA at the end of the span is ($L_{\text{span}} > 30$ dB)

$$\text{NF}_{\text{total}} = \frac{L_{\text{span}}}{G_{\text{FR}}} \left[\text{NF}_{\text{BR}} + \frac{\text{NF}_{\text{EDFA}} - 1}{G_{\text{BR}}} \right]. \quad (13)$$

The OSNR improvement for the case of 10 dB forward Raman gain and the backward Raman of case (c) is about 15 dB compared to the case without Raman (10 dB from the forward Raman). This comparison is not quite fair as it does not take into account the limitations in transmit power due to nonlinear penalties [18]. In the following sections, this effect will be taken into account.

D. Raman-Pumped ROPA

The addition of a ROPA in the middle of the span [at location "R" in Fig. 6(e)] improves the NF and OSNR significantly. The analysis of the span NF requires that the span be split into a Section I that includes forward Raman plus the span loss (L_1) to the ROPA, the ROPA gain and NF, and Section II that includes the backward Raman and span loss (L_2) from the ROPA to the span end. The total span loss is $L_{\text{span}} = (L_1 \cdot L_2)$ and the total NF using (9) is

$$\begin{aligned} \text{NF}_{\text{total}} = & L_1 \text{NF}_{\text{FR}} + \frac{\text{NF}_{\text{ROPA}} - 1}{G_{\text{FR}}/L_1} + \frac{L_2 \text{NF}_{\text{BR}} - 1}{G_{\text{FR}} G_{\text{ROPA}}/L_1} \\ & + \frac{\text{NF}_{\text{EDFA}} - 1}{G_{\text{FR}} G_{\text{ROPA}} G_{\text{BR}}/(L_1 \cdot L_2)}. \end{aligned} \quad (14)$$

Under the assumption that NF_{FR} is approximately $1/G_{\text{FR}}$, the formula simplifies to

$$\begin{aligned} \text{NF}_{\text{total}} = & \frac{L_1}{G_{\text{FR}}} \left[\text{NF}_{\text{ROPA}} + \frac{L_2 \text{NF}_{\text{BR}} - 1}{G_{\text{ROPA}}} \right. \\ & \left. + \frac{L_2 (\text{NF}_{\text{EDFA}} - 1)}{G_{\text{ROPA}} \cdot G_{\text{BR}}} \right]. \end{aligned} \quad (15)$$

The total NF is improved by placing the ROPA as far as possible from the fiber end which reduces the common factor L_1 while keeping the ROPA gain (G_{ROPA}) appreciably large. The ROPA position is limited by the amount of residual Raman pump power available (at least 5 mW is required). The ROPA NF (NF_{ROPA}) is about 5 to 5.5 dB typically. For a ROPA at 90 km from the fiber end with 20 dB of gain and the forward + backward Raman gain of the preceding example, the improvement in OSNR is about 27 dB (assuming a significantly long span). This comparison also needs to be adjusted for nonlinear penalties as will be discussed below. However, the relative improvement with the ROPA is about 12 dB compared to the case with forward and backward Raman and no ROPA.

Using any of the total NF equations above, the total OSNR can be calculated using (8)

$$\text{OSNR} = \frac{P_s \cdot G_{\text{total}}}{(G_{\text{total}} \cdot \text{NF}_{\text{total}} - 1) h \nu_s \Delta \nu} \quad (16)$$

where P_s is the signal transmit power into the span, $\Delta \nu$ equals 12.5 GHz for 0.1-nm bandwidth, and $G_{\text{total}} = G_{\text{FR}} \cdot G_{\text{ROPA}} \cdot G_{\text{BR}} \cdot G_{\text{EDFA}}/L_{\text{span}}$ for the last case discussed (OSNR measured after the final EDFA). If the total gain of all amplifiers compensates for the span loss, then $G_{\text{total}} = 1$.

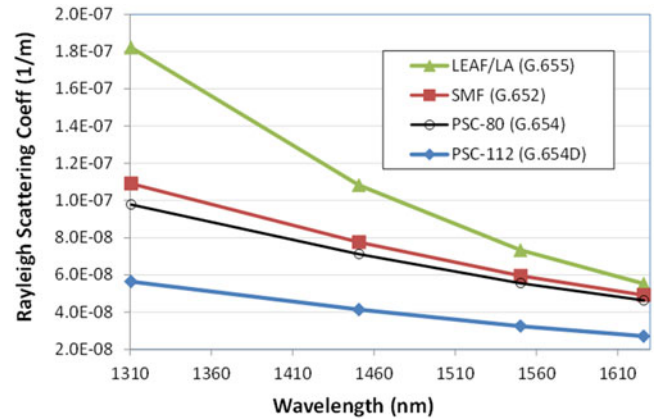


Fig. 8. Rayleigh scattering coefficient versus wavelength for several different fiber types (measured with an OTDR).

IV. RAMAN IMPAIRMENTS

The preceding section demonstrated the NF and OSNR improvements of Raman amplification. There are several effects that cause transmission penalties when using Raman that need to be considered.

A. Multiple-Path Interference (MPI)

Rayleigh scattering is a well-known effect in optical fibers and is a limiting factor for fiber attenuation. Signal light will back-scatter (opposite direction of the signal) during propagation and some of this back-scatter light will scatter again into the forward direction, called double Rayleigh scattering (DRS). Normally, this is a weak process, but coupled with the gain provided by Raman amplification, it can grow to become significant [19]–[22]. DRS is the main source of MPI and it can be assisted by discrete reflection points in the line system. The interaction length for DRS is many kilometers, so the DRS light is incoherent with the signal. Thus, the MPI light can be treated as an additional noise source. The Rayleigh scattering coefficient varies with different fiber types as shown in Fig. 8 and large A_{eff} PSC fibers have the lowest Rayleigh coefficient. The Rayleigh coefficient scales similarly to Raman gain in different fiber types (compare Figs. 2 and 8).

The MPI is a ratio relative to the signal power, so it appears like $1/\text{OSNR}$. In practice, the MPI should be kept below -20 dB. Since the MPI is an incoherent process, it adds up linearly versus the number of gain stages. This addition restricts the MPI to a lower value per span since, for example, 20 spans (13 dB) add 13 dB to the MPI value per span. This restriction further limits the amount of Raman gain that can be used to about 25 dB. The MPI for Raman gain less than 15 dB is fairly insignificant. One further interesting case is that of Raman and ROPA since the ROPA gain adds to the generation of MPI. Quite often (but not always!) a ROPA is designed with an isolator that eliminates the preceding back-scatter.

B. Polarization-Dependent Gain (PDG)

Raman amplification is a polarization-dependent process and requires equal pump power in orthogonal polarization states

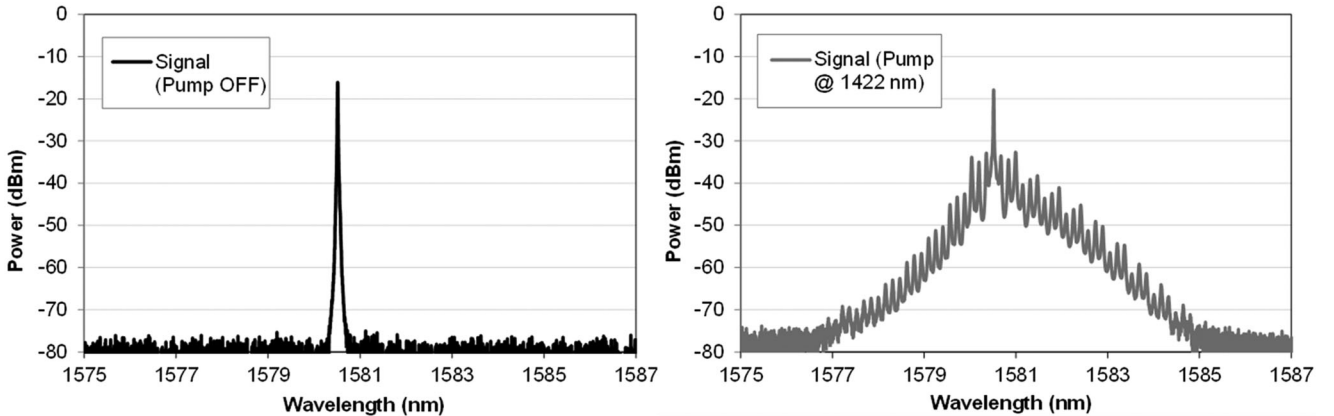


Fig. 9. FWM in LEAF fiber with ZDW near 1500 nm and signal near 1580 nm with no pump (left); and with forward pump at 1422 nm (right).

or de-polarization of a single pump to reduce PDG [23]. One important manufacturing aspect for dual-polarized pumps is to calibrate the pump power entering the fiber for each pump laser. The pump multiplexing scheme has polarization-dependent loss which can be compensated during the calibration process.

Polarization mode dispersion (PMD) and PDG are statistically coupled during propagation [24], [25] resulting in a Gaussian distribution in gain for low PMD fiber. There will be a larger variation in gain due to PDG in the forward Raman case compared to backward Raman [24]. For dual-polarized signals, the gain compression in forward Raman is also polarization dependent such that higher gain along one polarization state will result in higher pump depletion which has the effect of reducing the difference in pump power between each polarization state.

The penalties caused by PDG depend on the transponder sensitivity to this effect. At least one supplier of 100G coherent OIF modules has a specification of < 0.5 dB OSNR penalty for 3 dB of PDG or PDL.

C. Four-Wave Mixing (FWM) With Raman Pumps

FWM is a nonlinear process whereby four optical waves (some of which may be degenerate) couple through the third order susceptibility, $\chi^{(3)}$ [26], [27]. Conservation of energy ($\nu_1 + \nu_2 = \nu_3 + \nu_4$) and phase-matching conditions ($\beta_1 + \beta_2 = \beta_3 + \beta_4$) determine whether FWM process is significant. The process of interest for Raman is the mixing of three photons that transfer their energy to a fourth photon ($\nu_1 + \nu_2 - \nu_3 \rightarrow \nu_4$). The phase-matching requirements generally necessitate that the wavelengths involved are located on both sides of the zero-dispersion wavelength (ZDW) in the fiber. This occurs in NZDSF fibers with a ZDW near 1500 nm where Raman pumps are in the 1400 to 1510 nm range and signals in the 1520 to 1620 nm range [28]. The FWM process can occur with either forward or backward Raman amplification.

In backward Raman pumping, FWM occurs when one Raman pump is near the ZDW and one pump is at a shorter wavelength. For example, two pump photons (ν_1, ν_2) at 1500 nm mix with a third pump photon (ν_3) at 1450 nm to generate a photon (ν_4) at 1553.6 nm when the ZDW is near 1500 nm. The

backward-generated FWM light Rayleigh-scatters into the forward direction in the C-band as a noise source for channels near that wavelength. The distribution of the ZDW in NZDSF fibers can be fairly broad, with a standard deviation of 5 nm or more. This FWM case is most relevant to wide bandwidth Raman amplification where long wavelength pumps provide gain in the L-band.

In forward Raman pumping, FWM occurs when two photons at a pump wavelength less than the ZDW mix with a signal photon longer than the ZDW, creating an additional photon at the signal wavelength. The generated light is already traveling in the forward direction, so even a weaker FWM process can be a source of noise. For example, two pump photons (ν_1, ν_3) at 1453 nm mix with a signal photon (ν_2) near 1550 nm to generate a photon (ν_4) near 1550 nm when the ZDW is about 1500 nm. An example of FWM in LEAF fiber is shown in Fig. 9 with a single signal and pump wavelength. The frequency difference between FWM products in the signal spectrum is equal to the mode spacing in the pump.

FWM is not an issue in Raman amplified systems if these few cases are avoided. Also if the FWM products are not within the signal band, then operating under these conditions may not present a problem.

D. Noise Transfer

Raman pumps are usually multiple frequency mode laser diodes with a spectral width of ~ 1 nm. As a result of the wider bandwidth, the relative intensity noise (RIN) of the Raman pump is much higher than a distributed feedback laser and is typically -110 to -120 dB/Hz. The RIN of a Raman fiber laser is increased due to the cascading effect [29].

It is possible as the pumps propagate with the signals to transfer some of this RIN to the signal through the Raman amplification process [30], [31]. RIN may also transfer between pumps before transferring to a signal so that multiple pump processes have also been studied [32], [33]. Noise can transfer through phase (as opposed to just intensity) which has received additional consideration in the literature [34], including polarization effects [35], for phase-modulated signals. The last study

was particularly relevant as it modeled the spectral and polarization properties of pump lasers as they are typically implemented which results in a larger RIN penalty than more simplistic models. Generally speaking, phase and intensity noise are coupled through transmission in the fiber.

Chromatic dispersion causes the pumps and signals to have different group velocities so that the pump and signal waves walk off during fiber propagation. Additionally, backward Raman pumps walk-off is much faster since the pumps and signals travel in opposite directions. These effects cause an averaging or low-frequency filtering to occur which restricts the magnitude of noise transfer. Thus, the backward and forward Raman RIN transfer is limited to kilohertz and tens of megahertz bandwidths, respectively. The Q penalty is generally negligible for backward Raman and on the order of 0.1 dB Q for forward Raman over a single span with the pump RIN value mentioned above [30]. RIN transfer for forward Raman amplification is one of the effects that limit how often forward Raman can be used in a multiple span transmission link.

E. Other Impairments

Further work is required to analyze a significant impairment in forward Raman amplified systems that results in systems utilizing dual-polarized phase-modulated signal formats. Raman pumps that have low walk-off with the signal mediate a cross-polarization penalty that was not detected in single-polarized 10G OOK signal formats (which has a polarization insensitive receiver). A similar effect was noted in [35] and was attributed to a pump-signal cross-phase modulation. This impairment limits the number of spans that could employ forward Raman amplification and the pump wavelengths that would be used.

V. NONLINEAR PROPAGATION IN RAMAN SYSTEMS

Section III demonstrated the NF and OSNR benefits of Raman amplification. These comparisons to EDFA-only amplification did not take into account the difference in nonlinear transmission penalty that occurs with Raman systems. In this section, we will provide an approximate model for calculating the nonlinear propagation penalties in dispersion-uncompensated coherent transmission systems.

A. Baseline Transmission Model

The development of coherent digital signal processing has allowed signal propagation through a fiber link without inline dispersion compensation. Analytic models have been developed [36]–[38] that provide relatively simple calculations of nonlinear transmission penalties. The baseline formula that will be considered is the Gaussian-Noise model [36] which calculates a nonlinear noise power, P_{NL} , for a single span

$$\begin{aligned} P_{NL}(f) &= P_s^3 \Delta\nu \frac{16}{27} \gamma^2 \\ &\cdot \int_{-\infty}^{\infty} \int_{-\infty}^{\infty} df_1 df_2 g(f_1) g(f_2) g(f_1 + f_2 - f) \Lambda(f_1, f_2, f) \\ \Lambda(f_1, f_2, f) &= \left| \int_0^L dz p(z) \exp[i4\pi^2 \beta_2 (f_1 - f)(f_2 - f) z] \right|^2. \end{aligned} \quad (17)$$

In (17) P_s is the transmit signal power into the span, $\Delta\nu$ is the noise bandwidth, γ is the fiber nonlinearity, $g(f)$ is the signal spectral density, $p(z)$ is the *normalized* power profile in the fiber, and β_2 is the dispersion coefficient. (The formula is written slightly differently than in the reference which the reader may consult for further details.) Without Raman, $p(z) = \exp(-\alpha_s \cdot z)$ and the integration is carried out analytically with several approximations to arrive at a simple formula [36]

$$P_{NL} = \frac{8P_s^3 \gamma^2 L_{s,\text{eff}}^2 \alpha_s \Delta\nu}{27\pi |\beta_2| B_{ch}^3} \operatorname{asinh} \left(\frac{\pi^2}{2\alpha_s} |\beta_2| B_{ch}^2 N_{ch}^{2B_{ch}/\Delta f} \right) \quad (18)$$

where the B_{ch} is the channel bandwidth (Hz), N_{ch} is the number of channels at frequency spacing Δf , and $L_{s,\text{eff}}$ is the same definition as (4) using α_s . Additional formulae are presented, but (18) will suffice as a reference for comparison to the case of Raman amplification.

Once P_{NL} has been calculated, an effective OSNR can be defined as

$$\text{OSNR}_{\text{eff}} = \frac{P_s}{P_{\text{ASE}} + P_{\text{MPI}} + P_{NL}} \quad (19)$$

where the MPI power has also been included as a noise term and $P_{\text{ASE}} = \rho_{\text{ASE}} \cdot \Delta\nu$.

The important term for Raman amplification is the integration of $p(z)$ which now must be carried out using the Raman signal power profile. The profile with Raman is much more complicated and a simple model has been proposed for backward Raman [39]. However, this model still requires a complex integration to be performed and does not take into account the scenario with multiple pump wavelengths (and the complex Raman power transfer between them).

B. Forward Raman Transmission Model

The complexity of the Raman propagation equation (5) does not allow for a simplified signal power profile to be estimated. However, a semi-analytic solution can be found by fitting the calculated forward Raman signal profile to a simple function:

$$p(z) = b_1 \exp(-\alpha_s z) - b_2 \exp(-\alpha_2 z). \quad (20)$$

An example of a forward Raman power profile and fit is shown in Fig. 10. (Note that the fit function and calculations are in linear units and Fig. 10 is in logarithmic units.) The signal power profile has been normalized to 1 mW (0 dBm) at $z = 0$. The fit process is quite simple as α_s is the fiber attenuation and b_1 is the extrapolation of the fiber attenuation line that matches the signal profile after the Raman gain has become insignificant and is equal to the linear forward Raman gain. The first exponential of (20) is shown as a dashed line in Fig. 10. Then $b_2 = b_1 - 1$ (so that $p(0)$ is normalized 1 mW) and α_2 is chosen to give the same maximum signal power in the line.

This simple fit procedure results in a power profile that only has an error of a few percent when integrated over the fiber length compared to the original integrated signal profile. The benefit of this fitting function is that the fit function (20) can be substituted into (17) and solved in the same manner as the non-Raman signal profile. When the integration function (Λ) is squared, three terms result and simple substitution into (18)

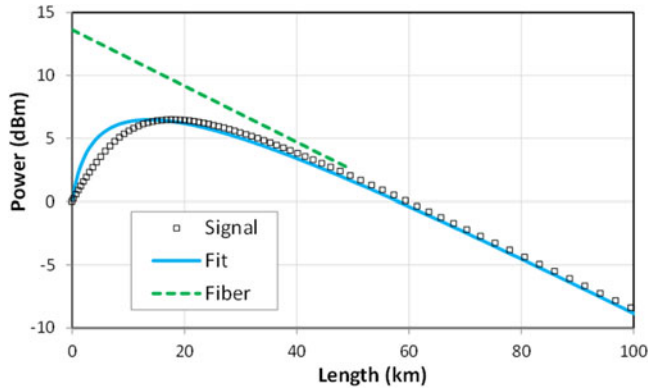


Fig. 10. Forward Raman signal profile (squares), fit (solid line), and first exponential term of fit (dashed line). The Raman gain is 13 dB.

TABLE I
SUBSTITUTION TERMS FOR FORWARD RAMAN

Original Term	Term 1	Term 2	Term 3
$L_{s,\text{eff}}^2$	$(b_1 L_{s,\text{eff}})^2$	$(b_2 L_{2,\text{eff}})^2$	$-2(b_1 L_{s,\text{eff}}) \cdot (b_2 L_{2,\text{eff}})$
α_s	α_s	α_2	$\sqrt{\alpha_s \alpha_2}$

is possible. The three substitution terms are shown in Table I, where $L_{s,\text{eff}}$ is defined with α_s and $L_{2,\text{eff}}$ is defined with α_2 . The solution is then a sum of three terms equivalent to (18) with the above substitutions:

$$P_{\text{NL-FR}} = \sum_{i=1}^3 P_{\text{NL}}(L_{i,\text{eff}}^2, \alpha_i) \quad (21)$$

where $L_{i,\text{eff}}^2$ and α_i correspond to the three terms in Table I.

Now the comparison between forward Raman and no Raman can be made by choosing a transmit power without Raman that gives the same P_{NL} as with forward Raman. Eventually, it is OSNR_{eff} that needs to be calculated, so these comparisons of P_{NL} must be scaled to the same signal power. Thus, the quantity P_{NL}/P_s needs to be compared.

For the power profile of Fig. 10, the transmit power without Raman with the same P_{NL}/P_s is about +8.0 dBm. To achieve the same OSNR as the Raman profile, the transmit power would need to be +13 dBm (as shown by the dashed line in Fig. 10). Thus, the OSNR benefit of forward Raman in this case is about 5 dB at the same P_{NL} . The nonlinear power with forward Raman depends to a larger extent on the maximum power in the fiber, but there is also a dependence on the Raman gain. The same maximum power in the fiber can be achieved with higher transmit power and lower Raman gain. There is no simple rule that can be applied to determine the transmit power without Raman that gives the equivalent amount of P_{NL}/P_s . In general, the effective OSNR benefit in dB is $G_{\text{FR-dB}} - \Delta P_{\text{dB}}$, where ΔP_{dB} is the difference in transmit power (in dB) without Raman to achieve the same P_{NL} . One example of a plot of OSNR benefit with forward Raman relative to transmitting without Raman at the same P_{NL}/P_s is shown in Fig. 11 calculated for a single signal in SMF. It should be pointed out that for a large number of signals, the power in the fiber without Raman may be limited by

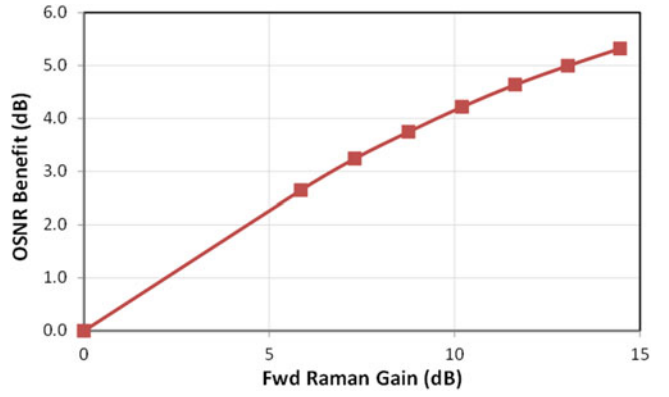


Fig. 11. Forward Raman OSNR benefit normalized to the same P_{NL} as without Raman in SMF.

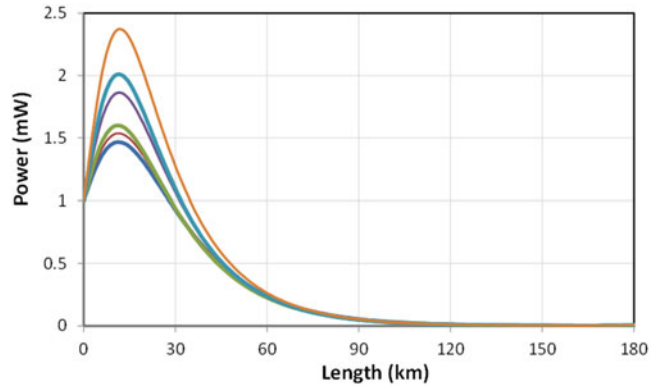


Fig. 12. Forward + backward Raman signal profiles in mW for 6 channels spread across the C-band and with 3 pumps (the same variation occurs for a fully occupied C-band channel plan).

the transmit amplifier. In this case, ΔP_{dB} is lower due to these practical constraints and the OSNR benefit of Raman is larger.

One further important point is that with Raman, the power profile may be very different for each signal. An example of multiple signals in the C-band with forward Raman amplification (3 pumps) is shown in Fig. 12. This variation in signal power profiles requires that the fit function (20) be calculated on a per-signal basis. P_{NL} should also be calculated on a per-signal basis as described in [36] rather than using the simpler formula (18). One possible simplification is to average the forward Raman signal profiles and use just a single fit function with (18) and (21) which is in reasonable agreement with the more accurate per-channel method.

C. Backward Raman Transmission Model

Similar to the forward Raman case, a semi-analytic solution can be found by fitting the calculated backward Raman signal profile to a simple function

$$\begin{aligned} p(z) &= \exp(-\alpha_s z) + b_2 \exp[-\alpha_2(L-z)] \\ &= \exp(-\alpha_s z) + b_2 \exp(-\alpha_2 L) \exp(+\alpha_2 z) \end{aligned} \quad (22)$$

where the first exponential is the standard fiber attenuation and b_2 is the backward linear Raman gain, and α_2 is chosen for

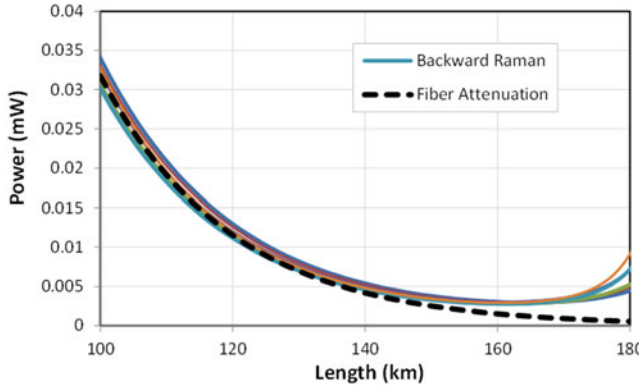


Fig. 13. Backward Raman signal profiles of Fig. 12 showing the backward Raman gain (~12 dB) relative to the fiber attenuation (without backward Raman).

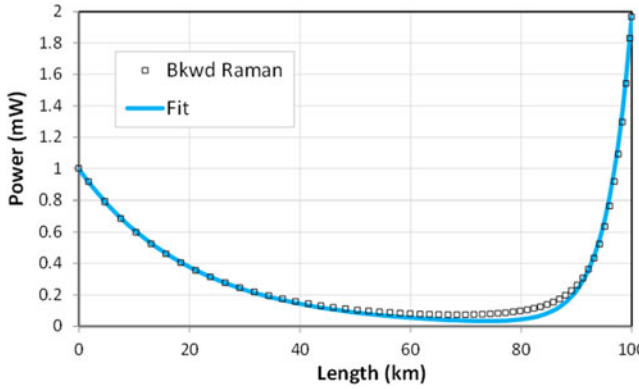


Fig. 14. Strong backward Raman signal profile in mW and 2-exponential fit.

best fit. This function can similarly be substituted and solved for as was described in the previous section. However, this is generally not required as the backward Raman power profile does not make a significant difference in the calculation of P_{NL} if the output power of the span is 13 dB below the maximum power within the span. This is almost always the case since backward Raman is only used on longer spans.

The signal power profiles in Fig. 12 also include the same Raman pumping in the backward direction as the forward direction. On a linear scale, the effect of backward Raman on the integrated power profile is negligible. The backward Raman gain may be seen by expanding the scale of Fig. 12 near 180 km as shown in Fig. 13 where the deviation from the dashed line is due to backward Raman gain. The conclusion is that weak backward Raman amplification does not significantly increase P_{NL} . The case of a ROPA with backward Raman is also typically insignificant as with larger span loss, the amplified signal power profiles are only a minuscule fraction of the transmitted signal power.

Strong backward Raman may occur on shorter spans with larger Raman gain, possibly enough such that no discrete amplifiers are needed in line [40]–[42]. An example of a strong backward Raman signal profile is shown in Fig. 14 and the fit from equation (22). In this case, the output power from the span is greater than the input power to account for losses of the

Raman module and other passive optical components. Even so, the area under the curve for $z > 80$ km is about 40% of the area under the curve in the first 80 km.

The high OSNR from this configuration allows the transmit power into the span to be lower. The rough scaling of P_{NL}/P_s is $(P_s^2 \cdot \text{Area}^2)$ so that transmitting at 2 dB lower power results in less than 80% ($0.63^2 \cdot 1.4^2$) of the nonlinear power. Thus, the OSNR_{eff} is higher than for the same span with weak backward Raman and an EDFA. Consequently, strong backward Raman has the potential for long transmission distances.

VI. IMPLEMENTATION OF RAMAN AMPLIFICATION

There are several important issues for the implementation of Raman amplifiers in telecommunications networks including design, installation, and operational aspects. In the following sections the essential features of implementation will be discussed.

A. Amplifier Design

A Raman amplifier comprises several key elements: a multiplexer to combine the Raman pumps with the signals, a pump isolator to eliminate any optical feedback that might destabilize or damage the pump lasers, a pump de-polarizing technique, and a spectral monitor to control the pumps. Additionally, the Raman pumps have enough optical power such that a robust safety mechanism must be employed that includes shuttered high-power optical connectors. Expanded-core connectors offer the highest optical power rating. The reliability of 14xx-nm laser diodes is very high with field data of 2.8 FIT being reported [43].

In Section IV-B, the importance of minimizing polarization-dependent gain was discussed. Laser diodes are typically used as the Raman pumps and the optical power is monitored by an internal photodiode that measured leaked light from the back facet. The relationship between output power and back-facet power is not completely linear. Thus, when combining two orthogonally-polarized pumps, it is important that the power of each polarization coming out of the amplifier be calibrated over the full operating range.

The spectral monitor is important both for pump control and for the detection of loss-of-signal (i.e., a fiber cut) for automatic laser safety shutdown. Both of these issues will be discussed in the following sections.

B. Control of Raman Pumps

The method of control of the Raman amplification process is one of the most critical issues for operational implementation. Raman gain can be controlled in a simplistic way by noting that the gain in dB is directly proportional to the total pump power in mW (see Fig. 5). One difficulty for distributed Raman is that there is no direct measurement of the input power as in a discrete amplifier (other than from embedded information that is passed down from the preceding network node). Thus, the gain is not well defined—especially when the line fiber loss may vary over time. Another possibility is to filter out part of the ASE spectrum

as the ASE power in dBm is approximately proportional to the Raman gain in dB. In either case, all the Raman pumps would have to be adjusted in unison which gives no control over the spectral shape.

A better and more powerful method is to control the amplified output power spectrum [44] as this can be directly monitored within the Raman amplifier module. This requires that the spectral monitor is capable of making at least a coarse measurement of the entire signal spectrum. Power control allows the Raman amplifier to compensate for changing line conditions which cause the fiber loss and spectral shape to vary. The most flexible approach to controlling the power spectrum is to dynamically control the power of each pump wavelength.

This is a somewhat complex optimization problem since the Raman equations are nonlinear and coupled with constraints on the dynamic range of the pump power. In addition, it is desirable to control the parts of the spectrum in which there are no signals such that turning up signals in a new spectral region does not cause a major adjustment in the pump settings. Dynamic control of an all-Raman amplification system has been continuously operating in the field with high reliability and stability [45] for over ten years. Examples of spectral control and stability with Raman amplification in field trials have been previously reported [40], [46].

Forward Raman amplification has no real-time feedback in order to adjust the pumps. This constraint suggests a feed-forward approach where the Raman pumps are adjusted based on an algorithm that tries to maintain constant gain as a function of the aggregate input signal power.

C. Optical Connectors and Fiber Losses

One issue of concern for the installation of distributed Raman amplifiers are optical connectors and other lumped fiber losses. The power handling specification for standard optical connectors is about 250 mW which is below the power typically used for Raman amplification. The damage mechanism in fiber optic connectors is either caused by dielectric breakdown (for pulsed laser systems) or thermal mechanisms [47]. Thermal damage is caused by the absorption of optical power by surface contaminants. In the worst case, severe defects in the fiber can cause a “fiber fuse” effect in which damage back-propagates toward the laser source [48].

In reality, the power handling value depends on the core surface quality of the connector which is difficult to specify. A recent field trial on aged metro fiber [40], [41] with over 100 standard SC connectors was demonstrated using high power (>1800 mW) distributed Raman amplification in every span without any connector damage. Thus the issue of optical damage becomes a risk assessment based on the installation and maintenance operating procedures (connector inspection and cleaning). The risk of damage can be greatly reduced by using a fiber connector with an expanded core such that the optical intensity is reduced. Some commercial high power / expanded-core optical connectors have damage threshold of 3000 mW or more.

Optical lumped losses due to connectors or poor quality fiber repairs or routing result in a loss of Raman gain. For losses

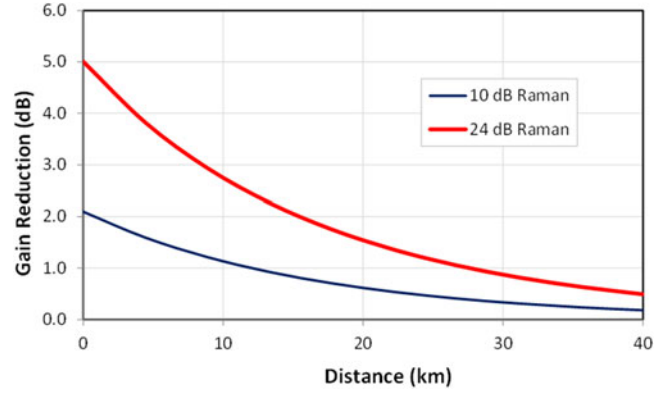


Fig. 15. Raman gain reduction with a 1 dB loss versus loss distance (not including the 1 dB loss of signal power) for a Raman gain (without loss) of 10 dB and 24 dB.

in the immediate vicinity of the Raman amplifier module (i.e., connector loss at an optical distribution panel) the loss of gain is easy to calculate. Suppose the Raman gain in dB is G_{dB} with a Raman pump power in mW of P_{mW} . A connector transmission ($T_{\text{loss}} < 1.0$) reduces the pump power to $P_{\text{mW}} \cdot T_{\text{loss}}$ resulting in a Raman gain of $G_{\text{dB}} \cdot T_{\text{loss}}$. For example, a gain of 10 dB is reduced to 7.9 dB with a loss of 1 dB ($T_{\text{loss}} = 0.79$). There is also an additional loss of the signal power by 1 dB. The reduction in pump power at all wavelengths may also result in a change in the shape of the gain spectrum. The loss of Raman gain diminishes as the distance of the loss from the Raman amplifier increases. Fig. 15 shows a plot of backward Raman gain reduction versus the location of a 1-dB loss. The effect of the loss is noticeable out to 30 or 40 km based on the maximum Raman gain.

D. Transient Events

A transient event is a sudden change in optical power level, usually due to a fiber cut that removes a fraction of the number of channels. An amplifier that operates in the pump depletion regime has a gain that is dependent on the signal loading power [14]. The gain is lower at higher input signal power and therefore a loss of input signal power will cause the gain to increase. This effect is quite well known in EDFAs where there is a high amount of gain compression [49], [50].

In Raman amplifiers, transient power fluctuations have also been studied [51]. A simple way to estimate the gain variations is to consider the ratio of amplified signal photons to pump photons (the photon ratio). For backward Raman amplification this is

$$PR = \frac{P_s(L)/\nu_s}{P_p(L)/\nu_p} \quad (23)$$

where $P_s(L)$ and $P_p(L)$ are the total signal and pump power at the end of the fiber, respectively. As an example, 100 signals centered at 1550 nm with an output power of -20 dBm/ch has a total output power of 0 dBm (1 mW). For backward Raman with a total pump power of 500 mW at 1450 nm, the photon ratio is 0.2%. This small ratio means that the gain compression is very small for this example and therefore the Raman gain is relatively independent of the number of signals. The lower efficiency of backward Raman becomes

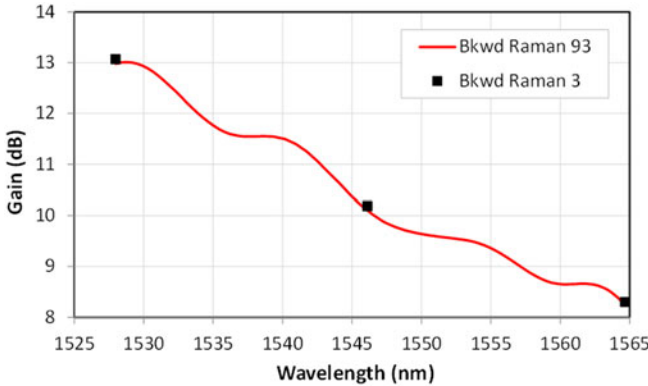


Fig. 16. Raman gain for 93 channels (lines) and 3 channels (squares) at the same pump power for backward (left) and forward (right) pumping. For forward pumping the corrected gain for 3 channels is also shown (circles).

a benefit for transient control. An example of the backward Raman gain for 93 and 3 channels in the C-band is shown in Fig. 16 (left).

For forward Raman amplification, the photon ratio is much higher. This is a more difficult case to estimate since the signal power is increasing while the pump power is decreasing with distance in the fiber. For the example of Fig. 12 at 10 km within the fiber, the photon ratio might be 40% for 100 signals and 3 pumps. This results in a gain compression of approximately $10 \cdot \log_{10}(1 - 0.4) = 2.2$ dB (an accurate value needs to be calculated by solving the Raman equations). This is still a much smaller value than for EDFA which often operate in the power saturated regime, meaning that the output power is approximately constant independent of the number of signals. In this case an EDFA with 100 signals will have an increase in gain of 10 dB if the number of signals drops to 10 (100/10 in dB). As mentioned in Section VI-B, the method to control forward Raman pumps must implement an algorithm based on input signal power which may be implemented in sub-microsecond timescales [52]. Thus a sudden change in input signal power will trigger a calculated change in pump power at approximately the same gain. An example of the forward Raman gain for 93 and 3 channels along with the corrected gain for 3 channels is shown in Fig. 16 (right).

E. Laser Safety

Raman amplifiers should comply with ITU-T recommendations for laser safety [53] and with the class 1M hazard level according to IEC [54] standard 60825-2 which requires a method to detect a line fiber cut or disconnected fiber jumper. A fiber optic telecommunications link typically includes a node-to-node optical supervisory channel (OSC). Thus a fiber discontinuity will result in both a loss of signal and loss of OSC which would trigger an automatic shutdown or automatic power reduction of the Raman pump lasers. A forward Raman amplification module is blind to fiber cuts in the following span and must receive signaling to shut down from other amplifier modules. All signaling and loss detection should be local as opposed to originating from remote sources (transponder receiver feedback) or over cabling that could be mistakenly disconnected. This limits the number of traffic affecting cables or connections.

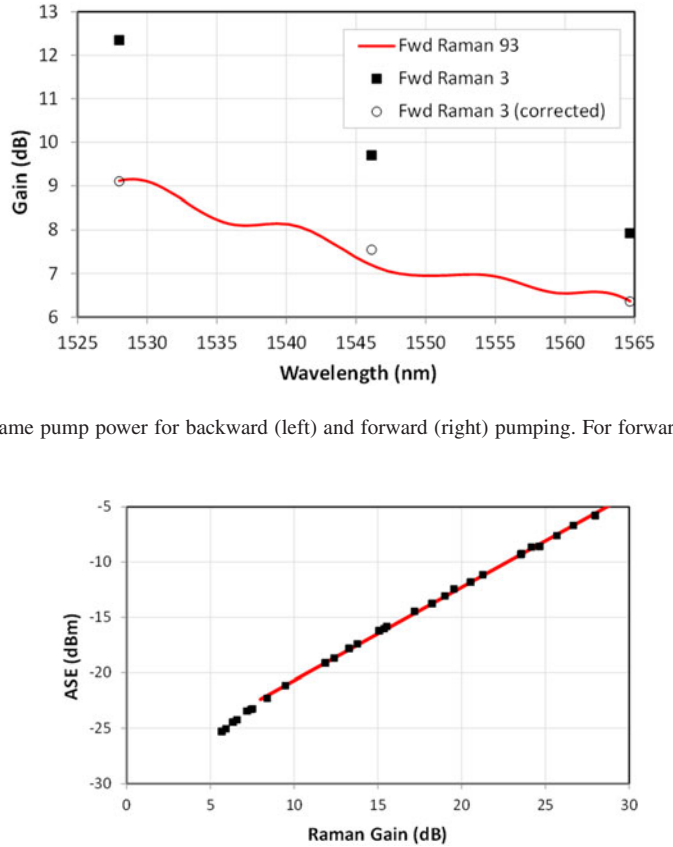


Fig. 17. ASE (dBm) generated from one fiber span versus Raman gain (dB) calculated (squares) over several fiber types of several attenuations each and fit to a line.

One case that needs to be considered is a long fiber span in which there are only one or a few signals with backward Raman amplification. The ASE in dBm that is generated over the C-band from the Raman module is proportional to the Raman gain in dB as shown in Fig. 17. For strong Raman gain, the ASE may be as high as -8 dBm (Raman gain higher than 25 dB is typically not used due to MPI limitations). If the span signal output power is on the order of -20 dBm then the ASE power may be much larger than the signal power. The spectral monitor of the Raman module must be able to detect this loss-of-signal in the presence of this strong ASE background. This may be accomplished by filtering the spectrum into smaller bands each of which is monitored by a separate photodiode. This type of spectral monitor is also useful for control purposes.

The Raman system also needs to be able to turn back on autonomously after the fiber discontinuity has been repaired. Detection of signals or OSC can trigger this restoration process. For very long spans, the signal(s) may not be able to be detected without the Raman amplification turned on and this situation requires an OSC with excellent receive sensitivity or with a separate mode of operation that improves the sensitivity beyond what is capable at normal OSC communication data rates.

F. Network Design

Raman amplification may be deployed in a number of different configurations as shown in Fig. 6, but not every span requires

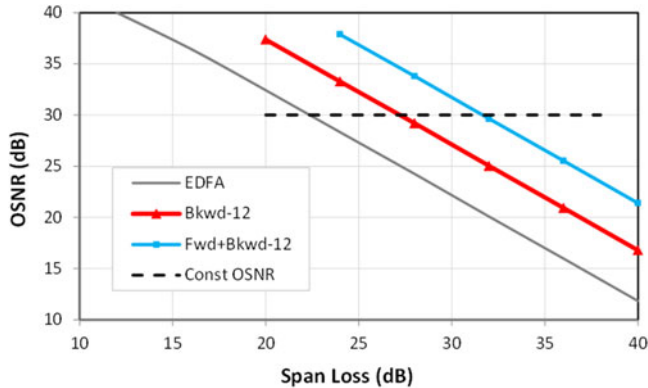


Fig. 18. OSNR plots versus span loss in SMF at a transmit power of 0 dBm/ch for EDFA, backward Raman (12 dB gain), and forward + backward Raman (12 dB gain each). The forward Raman transmit power is normalized for the same nonlinear power as transmitting at 0 dBm/ch without forward Raman.

Raman to economically improve performance. Unlike submarine repeatered systems, terrestrial systems are comprised of a variety of span lengths and occasionally different fiber types. The span loss in dB is proportional to the span length in km and the OSNR in dB without Raman is inversely proportional to the span loss in dB (assuming the same optical transmit power). The dB scaling is important as it means that a span with, for example, 6 dB higher span loss has an effect on the OSNR equivalent to 4 spans ($4 = 6 \text{ dB}$) at 6 dB lower loss.

A simple design strategy might be to target a similar range of OSNR values on all spans. This suggests a simple span loss threshold which employs higher performance Raman on higher loss spans. An example of this strategy is shown in Fig. 18 which displays OSNR plots for EDFA-only, backward Raman (12 dB gain), and forward + backward Raman (12 dB gain each). An OSNR threshold of 30 dB suggests the deployment of backward Raman at a span loss greater than 27.5 dB and forward + backward Raman at a span loss greater than 32 dB. This keeps the OSNR greater than 25 dB per span for span losses up to 37 dB (see Fig. 18).

For large A_{eff} fibers, the performance improvement from Raman is the same for the same Raman gain. The same gain will require higher Raman pump power that scales with A_{eff} (which in turn may require a higher power Raman module). Conversely, at the same Raman pump power, the gain in dB will scale inversely with A_{eff} (the same Raman module will be less effective at high A_{eff}).

The second important scaling rule is that the optimum maximum power in the fiber increases in large A_{eff} fiber. The OSNR improvement due to Raman is independent of the optimum transmit power since it depends only on Raman gain. Thus, an additional factor that must be considered is any limitations in transmit power. One hundred channels at +2 dBm/ch requires a +22 dBm transmit amplifier which is about the maximum for single-pump EDFA that are typically deployed. To achieve the benefit of large A_{eff} fiber may require a higher power EDFA to reach the optimum transmit power for longer spans. Forward Raman pumping requires less transmit power at the same non-

linear power limit and may allow a more optimum power profile if the transmit power is limited by the booster amplifier.

The other scaling factor to note is that the nonlinear power (P_{NL}) scales with the square of the fiber nonlinearity (γ) which further scales as $1/A_{\text{eff}}$. This nonlinear scaling is stronger than the performance improvement scaling of Raman. Thus, the best optical transmission performance with (or without) Raman is achieved with large A_{eff} fiber. In other words, smaller A_{eff} fiber with higher Raman gain does not result in better optical performance.

VII. SUMMARY AND CONCLUSION

A basic description of the Raman amplification process was provided including the scaling of Raman gain for different fiber types. The scaling laws also show that Raman gain in dB scales linearly with pump power in mW and inversely with fiber core effective area. The NF and OSNR benefit of Raman for different configurations were analyzed. The OSNR benefit must be considered in the context of the nonlinear transmission noise power and simple semi-analytic models were provided for both forward and backward Raman amplification. Additionally, transmission impairments specific to Raman were discussed which include noise transfer and multiple-path interference. The most common configuration of Raman, weak backward Raman amplification, was shown to have very low penalties, no significant increase in nonlinear power, and an improvement in OSNR that may allow three times or more maximum transmission distance.

A high spectral density modulation format such as 16QAM typically requires about 7.5 dB higher OSNR than QPSK. This factor is greater than 5 in linear units so that a transmission distance of 3000 km with QPSK compares to a transmission of <600 km with 16QAM. 16QAM, with one regeneration site, is a break-even with QPSK in terms of cost per capacity since 16QAM has twice the spectral density. However, this still only equates to less than 2/5 of the reach. The OSNR improvement that results from a Raman line system allows 16QAM to be used in long-haul networks at a lower cost per capacity × reach once a significant number of channels are deployed.

The implementation of Raman must consider the effect of lumped losses in the fiber plant and the risk of connector damage which can be mitigated with specially designed high power connectors. A dynamic control methodology for Raman amplification modules not only simplifies the operation, but tracks changes in the fiber plant over time. The fundamentals of laser safety and transient control were discussed. Raman systems have matured over the last decade and have demonstrated high reliability and flexibility in deployed networks.

The decision to employ Raman amplification ultimately depends on the cost advantages. High spectral density transponders with coherent receivers have greatly improved the capacity for data transmission. At the same time, these advancements have resulted in a cost structure heavily weighted toward transponder line cards and regeneration cards. The cost advantage of Raman is the reduction or elimination of transponder regeneration. The cost of a Raman-enhanced line system may be equivalent to just several regeneration channel cards. Thus, at higher

channel capacity the savings of regeneration cards will dominate the network costs resulting in a considerable reduction in total cost. Additionally, the cost of electrical power and cooling should be considered. A high power laser diode typically requires 10 W of electrical power and three of them are required to provide 10 to 12 dB gain in the C-band. In comparison, a coherent digital processor requires 80 to 100 W. Thus, six Raman modules have a similar power requirement as one regeneration card. So there is a substantial savings in power and operating costs by employing Raman to remove a regeneration site.

ACKNOWLEDGMENT

The author would like to thank his colleagues at Xtera Communications for their collaborations in the research and design of Raman systems. Specifically, he would like to thank D. Chang, S. Burtsev, P. Perrier, and H. Fevrier with whom he has worked for over 14 years.

REFERENCES

- [1] M. N. Islam, "Raman amplifiers for telecommunications," *IEEE Sel. Topics Quantum Electron.*, vol. 8, no. 3, pp. 548–559, May/Jun. 2002.
- [2] M. N. Islam Ed., *Raman Amplifiers for Telecommunications*. New York, NY, USA: Springer-Verlag, 2003.
- [3] J. Bromage, "Raman amplification for fiber communications systems," *J. Lightw. Technol.*, vol. 22, no. 1, pp. 79–93, Jan. 2004.
- [4] W. Pelouch, "Raman amplification: An enabling technology for high-capacity, long-haul transmission," presented at the Optical Fiber Communications Conf., Los Angeles, CA, USA, 2015, Paper W1C1.
- [5] R. Sutherland, "Stimulated Raman scattering" in *Handbook of Nonlinear Optics*, New York, NY, USA: Marcel Dekker, 1996.
- [6] R. H. Stolen, "Fundamentals of Raman amplification in fibers," in *Raman Amplifiers for Telecommunications*, M. N. Islam, ed., New York, NY, USA: Springer-Verlag, 2003.
- [7] K. Rottwitt and J. Pavlens, "Analyzing the fundamental properties of Raman amplification in optical fibers," *J. Lightw. Technol.*, vol. 23, no. 11, pp. 3597–3605, Nov. 2005.
- [8] J. Bromage, K. Rottwitt, and M. Lines, "A method to predict the Raman gain spectra of germanosilicate fibers with arbitrary index profiles," *Photon. Technol. Lett.*, vol. 14, no. 1, pp. 24–26, Jan. 2002.
- [9] N. Newbury, "Pump-wavelength dependence of Raman gain in single-mode optical fibers," *J. Lightw. Technol.*, vol. 21, no. 12, pp. 3364–3373, Dec. 2003.
- [10] S. Radic, "Forward, bidirectional, and higher-order Raman amplification," in *Raman Amplifiers for Telecommunications*, M. N. Islam, ed., New York, NY, USA: Springer-Verlag, 2003.
- [11] S. Papernyi, V. Karlov, and W. Clements, "Third-order cascaded Raman amplification," presented at the Optical Fiber Communications Conf., Anaheim, CA, USA, 2002, Paper FB4.
- [12] J. D. Ania-Castañón, "Quasi-lossless transmission using second-order Raman amplification and fibre Bragg gratings," *Opt. Exp.*, vol. 12, no. 19, pp. 4372–4376, Sep. 2004.
- [13] H. Bissessur, "Amplifier technologies for unrepeated links, submarine transmissions," presented at the Optical Fiber Communications Conf., Anaheim, CA, USA, 2013, Paper OTh4C3.
- [14] P. Becker, N. Olsson, and J. Simpson, *Erbium-Doped Fiber Amplifiers: Fundamentals and Technology*. San Diego, CA, USA: Academic, 1999.
- [15] E. Desurvire, *Erbium-Doped Fiber Amplifiers*. New York, NY, USA: Wiley, 1994, pp. 624–626.
- [16] S. R. Chinn, "Analysis of counter-pumped small-signal fiber Raman amplifiers," *Electron. Lett.*, vol. 33, pp. 607–608, Mar. 1997.
- [17] A. Kobyakov, M. Vasilyev, S. Tsuda, G. Giudice, and S. Ten, "Analytical model for Raman noise figure in dispersion-managed fibers," *Photon. Technol. Lett.*, vol. 15, no. 1, pp. 39–32, Jan. 2003.
- [18] P. Krummich, R. Neuhauser, H. Bock, W. Fischler, and C. Glingener, "System performance improvements by codirectional Raman pumping of the transmission fiber," in *Proc. 27th Eur. Conf. Optical Commun.*, 2001, pp. 114–115.
- [19] P. Hansen *et al.*, "Rayleigh Scattering limitations in distributed Raman pre-amplifiers," *Photon. Technol. Lett.*, vol. 10, no. 1, pp. 159–161, Jan. 1998.
- [20] P. Parolari, L. Marazzi, L. Bernardini, and M. Martinelli, "Double Rayleigh scattering noise in lumped and distributed Raman amplifiers," *J. Lightw. Technol.*, vol. 21, no. 10, pp. 2224–2228, Oct. 2003.
- [21] S. Lewis, S. Chernikov, and J. Taylor, "Characterization of double Rayleigh scatter noise in Raman amplifiers," *Photon. Technol. Lett.*, vol. 12, no. 5, pp. 528–530, May 2000.
- [22] S. Burtsev, W. Pelouch, and P. Gavrilovic, "Multi-path interference noise in multi-span transmission links using lumped Raman amplifiers," presented at the Optical Fiber Communications Conf., Anaheim, CA, USA, 2002, Paper TuR4.
- [23] T. Tokura *et al.*, "Pump light depolarization method for low PDG Raman amplification," presented at the Optical Fiber Communications Conf., Anaheim, CA, USA, 2002, Paper ThGG24.
- [24] H. Kee, C. R. S. Fludger, and V. Handerek, "Statistical properties of polarization dependent gain in fiber Raman amplifiers," presented at the Optical Fiber Communications Conf., Anaheim, CA, USA, 2002, Paper WB2.
- [25] Q. Lin and G. Agrawal, "Statistics of polarization-dependent gain in fiber-based Raman amplifiers," *Opt. Lett.*, vol. 28, no. 4, pp. 227–229, Feb. 2003.
- [26] G. Agrawal, *Nonlinear Fiber Optics*, 3rd ed. San Diego, CA, USA: Academic, 2001.
- [27] J.-C. Bouteiller, L. Leng, and C. Headley, "Pump-pump four-wave mixing in distributed Raman amplified systems," *J. Lightw. Technol.*, vol. 22, no. 3, pp. 723–732, Mar. 2004.
- [28] L. Leng *et al.*, "Experimental investigation of the impact of NZDF zero-dispersion wavelength on broadband transmission in Raman-enhanced systems," presented at the Optical Fiber Communications Conf., Atlanta, GA, USA, 2003, Paper WE4.
- [29] S. Babin, D. Churkin, A. Fotiadi, S. Kablukov, O. Medvedkov, and E. Podivilov, "Relative intensity noise in cascaded Raman fiber lasers," *Photon. Technol. Lett.*, vol. 17, no. 12, pp. 2553–2555, Dec. 2005.
- [30] C. Fludger, V. Handerek, and R. Mears, "Pump to signal RIN transfer in Raman fiber amplifiers," *J. Lightw. Technol.*, vol. 19, no. 8, pp. 1140–1148, Aug. 2001; "Erratum: Pump to signal RIN 980 transfer in Raman fiber amplifiers," *J. Lightw. Technol.*, vol. 20, no. 2, p. 316, Feb. 2002.
- [31] B. Bristiel, S. Jiang, P. Gallion, and E. Pincemin, "New model of noise figure and RIN transfer in fiber Raman amplifiers," *Photon. Technol. Lett.*, vol. 18, no. 8, pp. 980–982, Apr. 2006.
- [32] M. Mermelstein, K. Brar, and C. Headley, "RIN transfer measurement and modeling in dual-order Raman fiber amplifiers," *J. Lightw. Technol.*, vol. 21, no. 6, pp. 1518–1523, Jun. 2003.
- [33] Y. Zhu, X. Zhang, and G. Zhang, "Mean relative intensity noise transfer in fiber Raman amplifiers using multiple-wavelength pumps," *J. Lightw. Technol.*, vol. 25, no. 6, pp. 1458–1465, Jun. 2007.
- [34] J. Cheng, M. Tang, S. Fu, P. Shum, D. Wang, and D. Liu, "Relative phase noise-induced phase error and system impairment in pump depletion/nondepletion regime," *J. Lightw. Technol.*, vol. 32, no. 12, pp. 2277–2286, Jun. 2014.
- [35] C. Marinelli, L. Lorcy, A. Durécu-Legrand, D. Mongardien, and S. Borne, "Influence of polarization on pump-signal RIN transfer and cross-phase modulation in copumped Raman amplifiers," *J. Lightw. Technol.*, vol. 24, no. 9, pp. 3490–3505, Sep. 2006.
- [36] P. Poggiolini, G. Bosco, A. Carena, V. Curri, Y. Jiang, and F. Forghieri, "The GN-model of fiber non-linear propagation and its applications," *J. Lightw. Technol.*, vol. 32, no. 4, pp. 694–721 Feb. 2014.
- [37] R. Dar, M. Feder, A. Mecozzi, and M. Shtaif, "Properties of nonlinear noise in long, dispersion-uncompensated fiber links," *Opt. Exp.*, vol. 21, no. 22, pp. 25685–25699, Nov. 2013.
- [38] A. Carena, G. Bosco, V. Curri, Y. Jiang, P. Poggiolini, and F. Forghieri, "EGN model of non-linear fiber propagation," *Opt. Exp.*, vol. 22, no. 13, pp. 16335–16362, Jun. 2014.
- [39] V. Curri, A. Carena, P. Poggiolini, G. Bosco, and F. Forghieri, "Extension and validation of the GN model for non-linear interference to uncompensated links using Raman amplification," *Opt. Exp.*, vol. 21, no. 3, pp. 3308–3317, Jun. 2014.
- [40] D. Chang, S. Burtsev, W. Pelouch, E. Zak, H. de Pedro, W. Szeto, and H. Fevrier, "150 × 120 Gb/s field trial over 1,504 km using all-distributed Raman amplification," presented at the Optical Fiber Communications Conf., San Francisco, CA, USA, 2014, Paper TuB2.2.
- [41] T. J. Xia *et al.*, "Transmission of 400G PM-16QAM channels over long-haul distance with commercial all-distributed Raman amplification system

- and aged standard SMF in field," presented at the Optical Fiber Communications Conf., San Francisco, CA, USA, 2014, Paper Tu2B.1.
- [42] S. Burtsev *et al.*, "150 × 120 Gb/s transmission over 3,780 km of G.652 fiber using all-distributed Raman amplification," presented at the Optical Fiber Communications Conf., Los Angeles, CA, USA, 2015, Paper W3E5.
- [43] J. Yoshida *et al.*, "2.8 FITs of field reliability of 1480 nm/14xx-nm pump lasers," presented at the Optical Fiber Communications Conf., Los Angeles, CA, USA, 2015, Paper W2A2.
- [44] F. Xue, L. Xiaoming, Z. Wei, and P. Jiangde, "Investigation of dynamical pump control for backward-pumped fiber Raman amplifiers," *Opt. Commun.*, vol. 245, no. 1–6, pp. 211–225, Jan. 2005.
- [45] H. Fevrier and B. Clesca, "Flow of innovations from terrestrial to submarine networks," WDM & Next Generation Optical Networking, Nice, France, 2014.
- [46] D. Chen *et al.*, "New field trial distance record of 3040 km on wide reach WDM with 10 and 40 Gbps transmission including OC-768 traffic without regeneration," presented at the Optical Fiber Communications Conf., Anaheim, CA, USA, 2006, Paper PDP30.
- [47] R. Wood, *Laser Damage in Optical Materials*. New York, NY, USA: Adam Hilger, 1986.
- [48] Y. Shuto *et al.*, "Fiber fuse phenomenon in step-index single-mode optical fibers," *IEEE J. Quantum Electron.*, vol. 40, no. 8, pp. 1113–1121, Aug. 2004.
- [49] A. Bononi and L. Rusch, "Doped-fiber amplifier dynamics: A system perspective," *J. Lightw. Technol.*, vol. 16, no. 5, pp. 945–956, May 1998.
- [50] S. Pachnicke, P. Kurmmrich, E. Voges, and E. Gottwald, "Transient gain dynamics in long-haul transmission systems with electronic EDFA gain control," *J. Opt. Netw.*, vol. 6, no. 9, pp. 1129–1137, Sep. 2007.
- [51] M. Karásek and M. Menif, "Channel addition/removal response in Raman fiber amplifiers: Modeling and experimentation," *J. Lightw. Technol.*, vol. 20, no. 9, pp. 1680–1687, Sep. 2002.
- [52] X. Zhou, M. Feuer, and M. Birk, "Submicrosecond transient control for a forward-pumped Raman fiber amplifier," *Photon. Technol. Lett.*, vol. 17, no. 10, pp. 2059–2061, Oct. 2005.
- [53] ITU-T Recommendation G.664, "Optical safety procedures and requirements for optical transport systems," (2012). [Online]. Available: <https://www.itu.int/rec/T-REC-G.664/en>
- [54] International Electrotechnical Commission 60825-2:2004/AMD2:2010. [Online]. Available: <http://www.iec.ch>

Wayne S. Pelouch (M'03) was born in Libertyville, IL, USA, in 1965. He received the B.A. degree in Physics (Hons.) and B.S. degree from Northwestern University, Evanston, IL, USA, in 1987, and the Ph.D. degree in applied physics from Cornell University, Ithaca, NY, USA, in 1992. His thesis covered ultrafast lasers and nonlinear optical processes with applications in semiconductor physics. After graduation, he joined the University of New Mexico/Air Force Research Labs in Albuquerque, NM, USA, and then worked for the Lions Eye Institute in Perth, Australia, as a Laser Physicist. Subsequently, he joined Coherent Technologies in Lafayette, CO, USA, where he was Principal Investigator on a number of SBIR programs related to waveguide laser and amplifier technology. He is currently the Director of Photonics at Xtera Communications, Allen TX where he leads all Photonics activities including research, product development, and system network design. He has authored numerous publications and patents related to Raman technology.

Dr. Pelouch is a Member of the IEEE Photonics Society.